PVP2012-78301

FATIGUE LIFE OF THE STRAIN HARDENED AUSTENITIC STAINLESS STEEL IN SIMULATED PWR PRIMARY WATER

Kazuya TSUTSUMI
EDF R&D – MAI, Moret-sur-loing, France
Mitsubishi Heavy Industries,
Takasago, Hyogo, Japan

Nicolas HUIN
EDF R&D - MAI, Moret-sur-loing, France
Institut P', Université de Poitiers-ENSMA,
Chasseneuil du Poitou, France

Thierry COUVANT
EDF R&D – MAI, Moret-sur-loing, France

Gilbert HENAFF
Institut P', Université de Poitiers-ENSMA,
Chasseneuil du Poitou, France

Jose MENDEZ
Institut P', Université de Poitiers-ENSMA,
Chasseneuil du Poitou, France

Denis CHOLLET
EDF R&D – MAI, Moret-sur-loing, France

ABSTRACT

Over the last 20 years or so, many studies have revealed the deleterious effect of the environment on fatigue life of austenitic stainless steels in pressurized water reactor (PWR) primary water. The fatigue life correlation factor, so-called F_{en}, has been standardized to consider the effect on fatigue life evaluation. The formulations are function of strain rate and temperature due to their noticeable negative effect compared with other factors [1,2]. However, mechanism causing fatigue life reduction remains to be cleared.

As one of possible approaches to examine underlying mechanism of environmental effect, the authors focused on the effect of plastic strain, because it could lead microstructural evolution on the material. In addition, in the case of stress corrosion cracking (SCC), it is well known that the strain-hardening prior to exposure to the primary water can lead to remarkable increase of the susceptibility to cracking [3,4]. However, its effect on fatigue life has not explicitly been investigated yet.

The main effort in this study addressed the effect of the prior strain-hardening on low cycle fatigue life of 304L stainless steel (SS) exposed to the PWR primary water. A plate of 304LSS was strain hardened by cold rolling or tension prior to fatigue testing. The tests were performed under axial strain-controlled at 300 °C in primary water including B/Li and dissolved hydrogen, and in air. The effect on environmental fatigue life was investigated through a comparison of the F_{en} in experiments and in regulations, and also the effect on the fatigue limit defined at 10^6 cycles was discussed.

NOMENCLATURE

F_{en} : environmental fatigue life correction factor
N_{leak} : fatigue life of cylindrical specimen in water (cycles)
δ : residual ferrite (%)
SFE : stacking fault energy (mJ/m^2)
M_s : martensitic transformation temperature (°C)
M_{d30} : martensitic transformation temperature (°C)
$R\varepsilon$: strain ratio
DH : dissolved hydrogen content (cc/kg·H$_2$O)
DO : dissolved oxygen content (ppm)
$\Delta\varepsilon_t$: a total strain range (%)
$\Delta\varepsilon_p$: a non-elastic strain range (%)
$\Delta\varepsilon_e$: an elastic strain range (%)
T : temperature (°C)
$\Delta\varepsilon_t/2$: strain amplitude (%)
$\Delta\varepsilon_t/dt$: strain rate (%/s)

INTRODUCTION

Cyclic plastic strain can play an important role on fatigue life in the low cycle region in air, Therefore it is expected to be beneficial to use a hardened material which exhibits less plastic strain compared with an as-received one at the same strain amplitude.

Moreover, the effect of the strain-hardening prior to exposure to the primary water on fatigue life of austenitic

stainless steel has not necessarily been investigated, as shown SCC field.

Based on the above context, the authors have performed low cycle fatigue tests on the prior-hardened material 304L stainless steel in PWR primary water in order to investigate its effect on low cycle fatigue live and fatigue limit defined at 10^6 cycles.

EXPERIMENTAL PROCEDURE
Material
The material tested was a 304L stainless steel rolled plate, 2000*5000*30mm in the as-received size (Heat XY182), annealed at 1100°C and water-quenched. Chemical composition of the material is given in Table 1 and is in good agreement with nuclear French requirements RCC-M 220. Metallurgical properties such as residual ferrite (δ), stacking fault energy (*SFE*) and martensitic transformation temperatures (*Ms*, Md_{30}) are listed in **Table** 2.

Samples were cut from the original plate. Two samples were cold-worked by one-direction rolling up to 5% and 10% reduction of the thickness, respectively. The step size of the thickness reduction during cold-rolling was 0.5 mm. The last sample was tensioned prior to machining fatigue specimens. The final reductions of the thickness were 10.4% (TPNo.1630 MHI 02) or 10.0% (TPNo.1630 MHI 03). Both cold workings were conducted at room temperature (RT) and in ambient air.

Tensile properties at 300°C and RT under longitudinal (L) and transverse (T) directions of the plate are presented in **Table** 3. The mechanical properties of the as-received (AR) material met the RCC-M 3307 French requirements.

Table 1 - Chemical composition of Heat XY182.

Heat	C	Cr	Ni	Si	Mn	S	P	Mo	Cu	N
304L SS (XY182)	0.029	18.00	10.0	0.37	1.86	0.004	0.029	0.04	0.02	0.056
RCCM220	<0.03	17-20	8-12	<1	<2	<0.03	<0.045		<1	

Table 2 - Metallurgical properties of Heat XY182.

Heat	δ(%)	*SFE* (mJ/m^2)	M_s (°C)	M_{d30} (°C)
304L SS (XY182)	3.0	30	-274	13

Table 3 - Tensile properties of XY182.

|	T(°C)	Direction	Ys (MPa)	UTS (MPa)	EL (%)	E (GPa)
RCC-M 3307	20	T	>175	>490	>45	-
	350	T	>105	-	-	-
XY182 As-received	20	L	220	555	68	196
		L	220	560	66	188
		T	220	546	68	192
		T	215	533	66	187
	300	L	138	401	48	168
		L	139	404	48	190
		T	137	406	47	199
		T	136	402	46	196
XY182 5%Rolled	300	L	248	435	37	167
		L	252	431	33	166
		T	248	438	31	166
		T	253	431	33	166
XY182 10%Rolled	300	L	333	462	28	169
		T	320	468	30	170

Specimens
Figure 1 shows the configuration of the hollow cylindrical specimen which was used in simulated PWR primary water at 300°C. The length of the parallel parts at the center of the specimen was 30 mm and the gage length was 24 mm. The outer diameter was 12 mm and the wall thickness was 3 mm. Specimens were machined out from the center thickness of plates in the way that the lengthwise direction would match the rolling direction or the tensioning direction. In order to remove scratches caused by the machining, the outer and inner surfaces of specimens were polished in the axial direction using emery papers of #100, #240, #400 and #800.

Figure 2 shows the solid specimen used for tests in air. The procedure of machining specimens was the same as the hollow-type. The outer surface was polished in the axial direction using silicon made polishing paper #320, #500 and #800 in order to obtain the equivalent surface roughness to that on hollow type specimens.
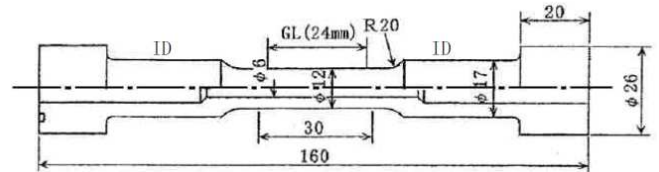
Figure 1 – Hollow-type specimen.
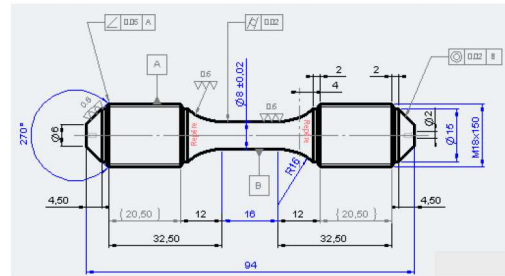
Figure 2 – Solid specimen.

Test apparatus

Figure 3 shows an outline of the test apparatus used for environmental experiments. Simulated primary water was pre-heated and circulated by a high-pressure pump through inside of the specimen. The average fluid velocity was 0.1m/s in the test section of the hollow cylindrical area. The temperatures on the outer and inner surfaces of test section were monitored by thermocouples, and the difference between them was assessed to be lower than 1°C. Tests were conducted with fully reversed axial strain-controlled (R_ε=-1), using a contact type extensometer attached to the outer surface of the specimen.

The test environment simulated PWR primary water with 1000 ± 100 ppm B as H_3BO_3, and 2 ± 0.2 ppm Li as LiOH, at 300°C. Dissolved oxygen (*DO*) was kept at < 5 ppb and dissolved hydrogen (*DH*) was kept at 30 ± 3 cc/kg·H_2O. All specimens were exposed to the environment about 24 hours prior to fatigue loading.

Tests in air were also performed under fully reversed axial strain-controlled, using a contact-type extensometer attached to the outer surface of the specimen. Temperature was monitored with thermocouples to make it stable.
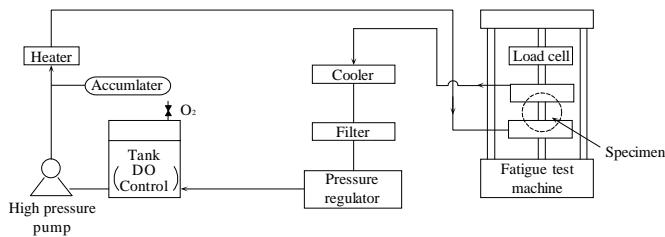

Figure 3 - Outline and overview of test apparatus.

Loading conditions

Table 4 and **Table** 5 give test matrixes for tests in simulated PWR primary condition and in air, respectively. Test parameters were the level of cold work (5% or 10%), the cold working process (tension or rolling) only in water, the strain rate in tension and the total strain amplitude. As reference, the as-received material was also tested. Strain rate in compression was kept at 0.4%/s. Two types of waveforms were applied; one was a triangle (strain rate 0.4%/s in tension) and the other was a saw tooth (strain rate 0.004%/s in tension). Strain amplitudes were selected as 0.15%, 0.25%, 0.35% and 0.50%.

Due to water contact at the inner surface of the hollow specimen, environmental fatigue cracks initiate on the inner surface and propagate toward the outer surface. For hollow specimens, fatigue life was defined as the number of cycles (N_{leak}) at which a fatigue crack penetrated through the wall thickness of the specimen.

Table 4 - Test Matrix in simulated PWR primary water.

TP-ID		Water chemistry	Temperature (℃)	Strain rate（%/sec）		Strain amplitude (%)
				in tension	in compression	
As received	1630 MHI 01	DO2＜0.005ppm DH=30cc/kg B=1000ppm Li=2ppm	300	0,4	0,4	0,5
	1630 MHI 04			0,004		
10% Tension	1630 MHI 02			0,4		
	1630 MHI 03			0,004		
5% Rolling	1630 MHI 05			0,4		
	1630 MHI 07			0,004		
10% Rolling	1630 MHI 11			0,4		0,5
	1630 MHI 12			0,4		0,35
	1630 MHI 13					0,25
	1630 MHI 17					0,15
	1630 MHI 14			0,004		0,5
	1630 MHI 15					0,35
	1630 MHI 16					0,25

Table 5– Test matrix in air.

TP-ID		Temperature (℃)	Strain rate（%/sec）		Strain amplitude (%)
			in tension	in compression	
As received	1630-95	300	0.4	0.4	0.5
10% Rolling	1630-40		0.4		0.5
	1630-41				0.35
	1630-42				0.25
	1630-46				0.15
	1630-45		0.004		0.5
	1630-44				0.35

TEST RESULTS

Results obtained in the primary water and in air are summarized in **Table** 6 and **Table** 7, respectively, along with EDF data collected in a previous work [5] on the same heat XY182 at the same temperature in the same environment using solid type specimens. In the present study, the maximum strain amplitude at which fracture of specimen did not occur up to 10^6 cycles was defined as the fatigue limit at 10^6 cycles.

Fatigue ε-N data in air and in water are presented in **Figure** 4, comparing the as-received with the cold-worked material. The ε-N curves evaluated with NUREG 6909 [1] and JSME code [2] are also reported in the figure. Almost all data are plotted on the ε-N curves drawn with regulations, demonstrating that these materials show similar fatigue lives.

Concerning the cold-working effect in air environment within a range of 0.2 - 0.5% strain amplitude, fatigue lives of the cold-worked material are shorter than those of the as-received one. Typically, for a strain amplitude of 0.5%, the fatigue life in the 10% cold rolled material is decreased by a factor of 2. In addition, there is no clear effect of strain rate on fatigue life in air on the cold-worked material. By contrast, for a strain amplitude lower than 0.2%, the cold-working prolonged fatigue lives and eventually leaded to an increase of the fatigue limit at 10^6 cycles, from 0.1% to 0.15%.

Figure 5 presents the evolution of plastic strain measured at mid life as a function of fatigue life in air. Difference in fatigue lives between materials still can be seen; so fatigue life in the range of 0.2 - 0.5% strain amplitude on the as-received material is not governed by plastic strain alone and it seems to be also depending on stress level during cycling.

Table 6 – Results obtained in PWR environment.

		TP-ID	Temperature (℃)	Strain rate (%/sec) in tension	Strain rate (%/sec) in compression	Strain amplitude (%)	Fatigue life (N)	Remarks
PWR	As received	1630 MHI 01	300	0,4	0,4	0,51	3114	
		1630 MHI 04		0,004		0,51	859	
		EDF-5-2		0,4		0,49	2729	
		EDF-5-10				0,5	3309	
		EDF-5-11				0,345	8341	
		EDF-5-19				0,35	10430	
		EDF-5-20				0,245	13889	
		EDF-5-22				0,2	32630	
		EDF-5-1				0,15	63000	
		EDF-5-23				0,1475	68109	
		EDF-5-34				0,125	110670	
		EDF-5-25				0,1	3437070	Run out
		EDF-5-39				0,103	1,00E+06	Run out
		EDF 5-29		0,004	0,004	0,5	1328	
		EDF 5-38				0,34	2781	
		EDF 5-33				0,25	6029	
	10% tension	1630 MHI 02		0,4		0,52	2224	
		1630 MHI 03		0,004		0,51	827	
	5% Rolling	1630 MHI 05		0,4		0,51	2870	
		1630 MHI 07		0,004		0,51	953	
	10% Rolling	1630 MHI 11		0,4	0,4	0,52	2590	
		1630 MHI 12				0,36	7361	
		1630 MHI 13				0,26	16634	
		1630 MHI 17				0,15	1,00E+06	Run out
		1630 MHI 14		0,004		0,51	887	
		1630 MHI 15				0,36	2162	
		1630 MHI 16				0,26	6864	

Table 7 – Results obtained in air.

		TP-ID	Temperature (℃)	Strain rate (%/sec) in tension	Strain rate (%/sec) in compression	Strain amplitude (%)	Fatigue life (N)	Remarks
AIR	As received	1630-95	300	0.4	0.4	0.5	9800	
		XADL-26				0.49	12520	
		XADL-104				0.395	19210	
		XADL-69				0.298	47470	
		XADL-45				0.249	57460	
		XADL-15				0.198	94530	
		XADL-49b				0.148	294300	
		EDF-7-1				0.5	12100	
		EDF-6-20				0.375	21500	
		EDF-6-19				0.25	55000	
		EDF-3-19				0.25	71815	
		EDF-6-12				0.25	47000	
		EDF-6-3				0.175	103000	
		EDF-4-19				0.175	119344	
		EDF-6-6				0.15	101000	
		EDF-6-13				0.125	396000	
		EDF-3-21				0.125	227438	
		EDF-5-41				0.1	1885001	Run out
	10% Rolling	1630-40		0.4		0.5	5400	
		1630-41				0.35	10000	
		1630-42				0.25	44000	
		1630-46				0.15	1.00E+06	Run out
		1630-45		0.004		0.5	4930	
		1630-44				0.35	15220	

On the contrary, in simulating PWR primary environment (**Figure** 4), fatigue lives of the cold-worked material were almost the same as those observed on the as-received one at strain amplitude above 0.2% irrespective of strain rate. This suggests that the loss of ductility induced by the prior cold-working does not necessarily reduce fatigue life in the primary water even at the low strain rate. Nevertheless, the fatigue limit at 10^6 cycles clearly increased up to the strain amplitude of 0.15% as observed in air.

Figure 6 presents the evolution of plastic strain measured at mid life as a function of fatigue life in PWR primary environment, suggesting that the plastic strain is the dominant factor driving fatigue life in both AR and cold-worked materials. This behavior is independent of the stress evolution during cycling

This very interesting finding could suggest that fatigue damage process, namely the underlying mechanism, should be different between these environments. **Figure 4** also indicates a

clear environmental effect on fatigue life even in the high cycle domain of around 10^5 cycles.
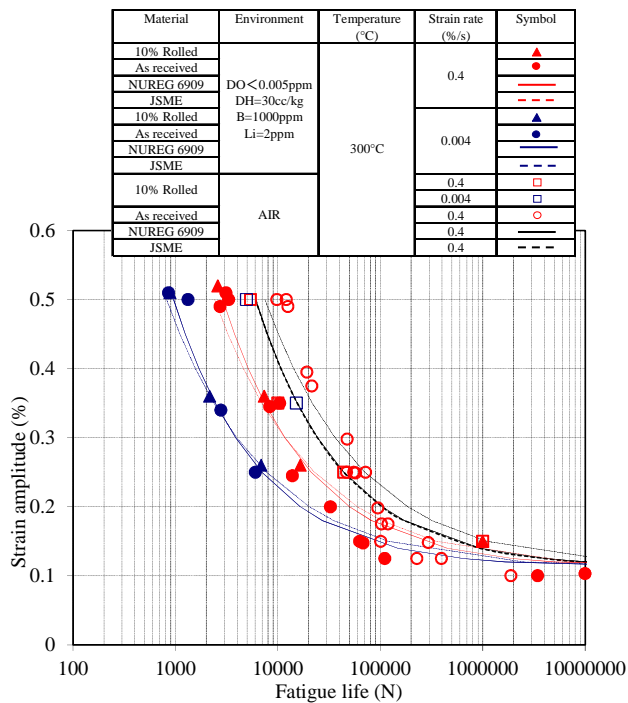
Material	Environment	Temperature (℃)	Strain rate (%/s)	Symbol
10% Rolled				▲
As received			0.4	●
NUREG 6909	DO＜0.005ppm			——
JSME	DH=30cc/kg			- - -
10% Rolled	B=1000ppm			▲
As received	Li=2ppm		0.004	●
NUREG 6909		300℃		——
JSME				- - -
10% Rolled			0.4	□
			0.004	□
As received	AIR		0.4	○
NUREG 6909			0.4	——
JSME			0.4	- - -

Figure 4 – Comparison between fatigue life in air and in PWR water at two levels of strain rate.

Material	Environment	Temperature (℃)	Strain rate (%/s)	Symbol
As receive	AIR	300℃	0.4	●
10% Rolled				■
			0.004	□
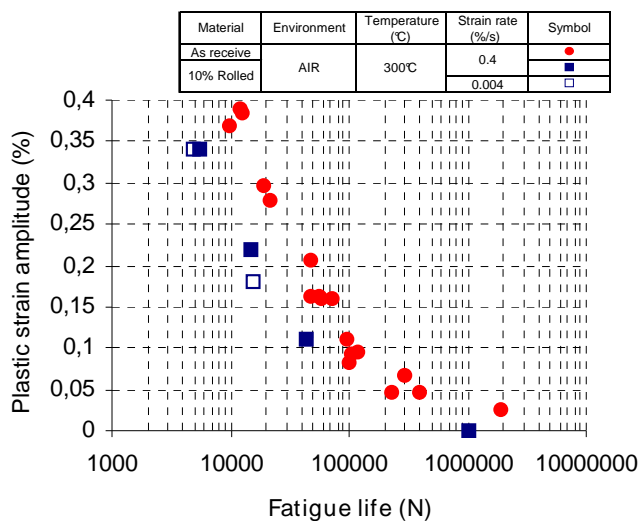
Figure 5 – Evolution of plastic strain measured at mid life as a function of fatigue life in air.

Material	Environment	Temperature (℃)	Strain rate (%/s)	Symbol
As receive	PWR	300℃	0.4	●
10% Rolled				■
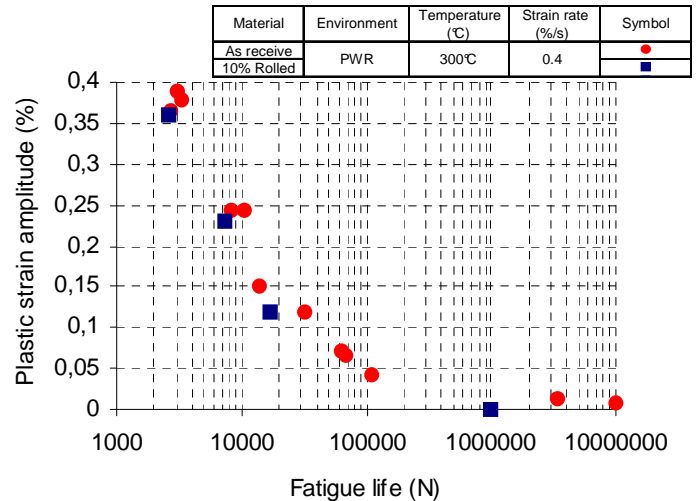
Figure 6 – Evolution of plastic strain measured at mid life as a function of fatigue life in PWR water.

DISCUSSION
Mechanical behavior during cycles

Figure 7 focuses on the effect of materials on the evolutions of the maximum stress at 0.5% strain amplitude. As shown here, there is a difference in hardening and/or softening behaviors: definite primary hardening can be observed only on the as-received material and a moderate hardening on the 5% rolled one and practically no hardening on the 10% rolled one, irrespective of strain rate condition. Nevertheless, an interesting point is that fatigue lives are almost the same in all materials in spite of the complete dissimilarity in the evolutions of the maximum stress. This fact suggests that fatigue life in PWR environment could be governed by local behavior (a crack initiates) rather than by the macro behavior of the material.

Figure 8 presents evolutions of the maximum stress on the cold-worked material tested in PWR water at several strain amplitudes from 0.15% to 0.52%. This figure reveals that all strain amplitudes, except for 0.15%, indicated hardening tendency only at the beginning (nearly up to 10 cycles) or almost no hardening, then followed by remarkable softening until the failure, irrespective of strain rate. At 0.15%, its stress level was nearly stable, meaning that neither hardening nor softening occurred. Regarding the effect of the strain rate on these evolutions, the low strain rate condition plotted with open symbols seemed to lead to more hardening. However, this tendency is only observed on one test. So, further investigations will be needed.

Figure 9 shows the evolution of the mean stress on the cold worked samples. At the lower strain rate, i.e. 0.15% and 0.26%, the mean stress of about 20-30 MPa was observed, but it seemed not to be deleterious enough to lead to fatigue life reduction. With increasing strain amplitude, the values decreased to nearly zero.
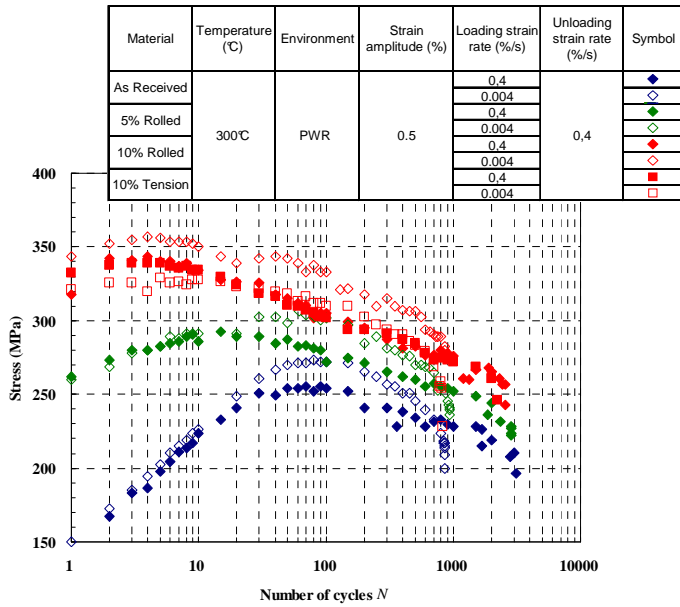
5   Copyright © 2012 by ASME

Material	Temperature (℃)	Environment	Strain amplitude (%)	Loading strain rate (%/s)	Unloading strain rate (%/s)	Symbol
As Received	300℃	PWR	0.5	0,4	0,4	◆
				0,004		◇
5% Rolled				0,4		◆
				0,004		◇
10% Rolled				0,4		◆
				0,004		◇
10% Tension				0,4		■
				0,004		□

Figure 7 - Evolution of the maximum stress as a function of number of cycles on the various materials.

Material	Environment	Temperature (℃)	Strain rate (%/s)	Strain amplitude (%)	Symbol
10% Rolled	O_2<0.005ppm DH=30cc/kg B=1000ppm Li=2ppm	300℃	0.4	0.15	◆
				0.26	◆
				0.36	◆
				0.52	◆
			0.004	0.26	◇
				0.36	◇
				0.51	◇

Figure 8 – Evolution of the maximum stress as function of number of cycles on the cold-worked material.

Material	Environment	Temperature (℃)	Strain rate (%/s)	Strain amplitude (%)	Symbol
10% Rolled	O_2<0.005ppm DH=30cc/kg B=1000ppm Li=2ppm	300℃	0.4	0.15	◆
				0.26	◆
				0.36	◆
				0.52	◆
			0.004	0.26	◇
				0.36	◇
				0.51	◇

Figure 9 - Evolution of the mean stress as function of number of cycles on the cold-worked material.

As a reference, the evolution of the mean stress at room temperature in air is shown in **Figure** 10 along with data obtained at 300 °C in air as well as in primary water. The value at room temperature is only significant, indicating that temperature highly affects the mean stress on the 10% rolled material. The mean stress of approximately 80 MPa at room temperature was good agreement with the literature data [6]. The mean stress seems not to be large enough to lead to fatigue life reduction in air at 300 °C.
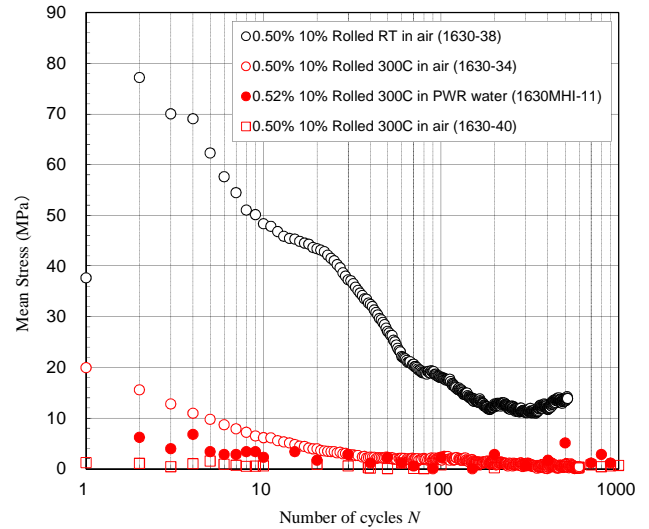

Figure 10 – Effect of temperature and test environment on the evolution of mean stress.
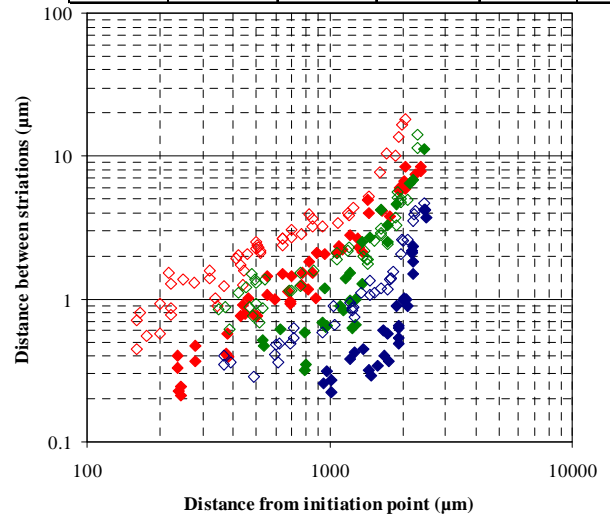
Crack propagations behaviors

In order to investigate the effect of cold working on crack propagation rate, distance between striations was measured on the fracture surface of the 10% cold-worked (tension and rolling) material and the as-received one, tested at strain amplitude of 0.5% in primary water. **Figure 11** shows the measured distance as a function of distance from the assumed initiation site, revealing that crack growth rates were accelerated with slowing strain rate, especially in small crack domain (<1mm). No difference was noticed between the cold-worked and the non cold-worked materials. It can be suggested that the cold working at least up to 10% does not lead to deleterious effect on the fatigue crack growth rate. It can be concluded that the equivalent fatigue life attributes the similar crack propagation life, deducing the similar crack initiation life as well.

Figure 12 indicates the effect of strain rate on crack growth rate at several strain amplitudes. It shows that a reducing strain rate leads to an increase of micro-crack growth rate up to a 1-2 mm depth for all considered strain amplitude. Results obtained at $\Delta\varepsilon_t/2 = 0.5\%$, $\Delta\varepsilon_t/dt = 0.4\%/s$ and at $\Delta\varepsilon_t/2 = 0.35\%$, $\Delta\varepsilon_t/dt = 0.004\%/s$, present not only similar crack propagation behavior but also similar fatigue lives which are respectively 2590 cycles and 2162 cycles. In the same way, for the two tests at $\Delta\varepsilon_t/2 = 0.35\%$, $\Delta\varepsilon_t/dt = 0.4\%/s$ and $\Delta\varepsilon_t/2 = 0.25\%$, $\Delta\varepsilon_t/dt = 0.004\%/s$ where fatigue lives are respectively 7361 cycles and 6864 cycles. **Figure 12** also highlights the fact that, for each strain amplitude, it was easier to observe a striation close to initiation sites at $\Delta\varepsilon_t/dt = 0.004\%/s$ than at $\Delta\varepsilon_t/dt = 0.4\%/s$, indicating the fact that even at the beginning of crack propagation, the main crack can advance more at the lower strain rate. This expectation is in good agreement with crack initiation observations, highlighting that a high strain rate results in a higher density of branched crack that may be, in that case, symptomatic of a reduction of the local mechanical loading.
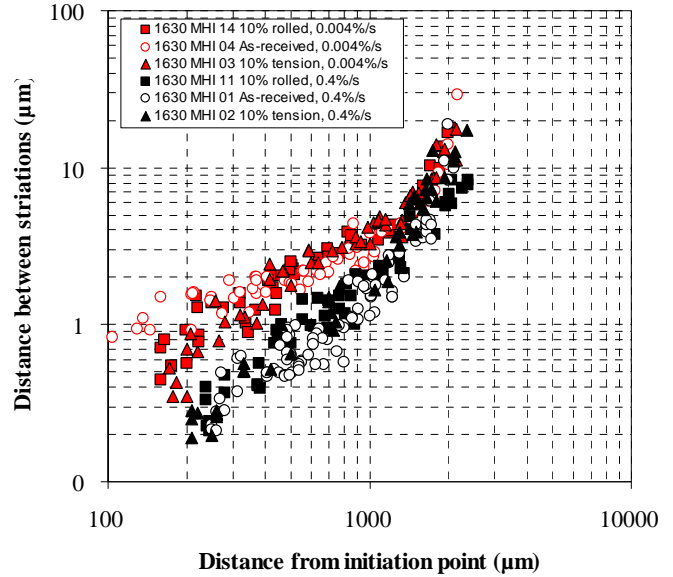
Figure 11 – Distance between striations as a function of distance from initiation point on the samples tested at strain amplitude of 0.5% in primary water.

Material	Environment	Temperature (°C)	Plastic strain at mid life (%)	Strain rate (%/s)	Symbol
			0.50	0.4	◆
			0.35	0.4	◆
10% Rolled	PWR	300	0.25	0.4	◆
			0.50	0.004	◇
			0.35	0.004	◇
			0.25	0.004	◇

Figure 12 - Distance between striations as a function of distance from initiation point on the 10% rolled material tested in primary water.

F_{en} evaluation

Figure 13 summarizes fatigue life as a function of the cold work level, confirming that fatigue lives in air clearly show its decreasing tendency when the cold-work level increases, whereas those in PWR water are almost equivalent irrespective of cold work level at both strain rate conditions.
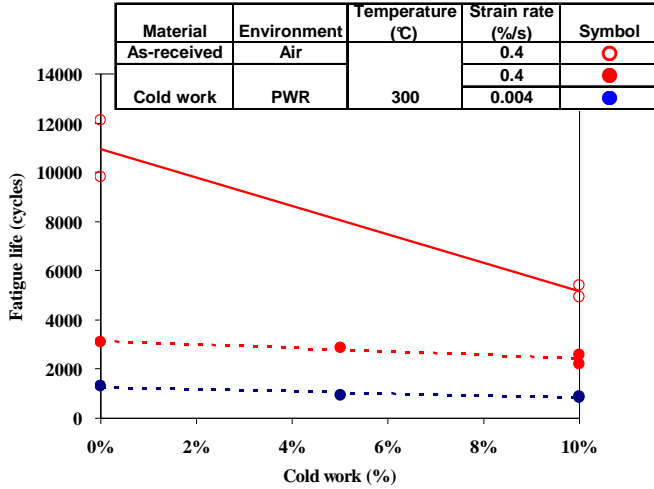

Material	Environment	Temperature (℃)	Strain rate (%/s)	Symbol
As-received	Air		0.4	○
			0.4	●
Cold work	PWR	300	0.004	●

Figure 13 – Fatigue life as a function of cold work level.

Figure 14 presents an evaluation of the experimental F_{en} as a function of strain rate. On each material, the F_{en} was calculated with fatigue life in air and that in the PWR primary water at the same strain amplitude. The evaluated F_{en} by NUREG 6909 [1] and the JSME code [2] are also given with the solid line and the dot line, respectively. It is clearly shown that F_{en} increases with decreasing strain rate whether or not the material was cold-worked, and F_{en} of the cold-worked material is almost half of that of the as-received one. As far as we only look at F_{en} values, it could be said that the environmental effect can be reduced by the cold-working (lower than 10%). Nevertheless, this difference is only due to the fact that fatigue lives of the cold-worked material in air are much lower than those of the as-received one, never meaning that a strain hardening lower than 10% can increase fatigue life compared with the as-received.

Regarding a comparison with the codifications, a tendency of the evaluated lines is in good agreement with the experimental F_{en}. Nevertheless, it can be noticed that NUREG 6909 evaluation is not enough restrictive for the as-received material, while the JSME code seems reasonable to predict environmental factors for the non cold-worked material and relatively conservative for the cold-worked one.
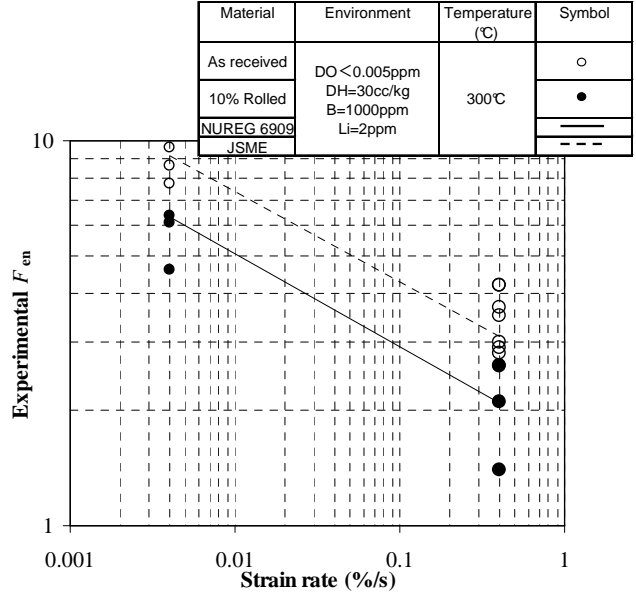

Material	Environment	Temperature (℃)	Symbol
As received	DO＜0.005ppm DH=30cc/kg B=1000ppm Li=2ppm	300℃	○
10% Rolled			●
NUREG 6909			——
JSME			– – –

Figure 14 - Experimental Fen for the cold-worked and the as-received materials in simulated PWR environment at 300°C.

Figure 15 and **Figure 16** present the comparison between the expected fatigue lives evaluated with NUREG 6909 [1] or JSME code [2], and the experimental fatigue lives obtained in this study. Both figures indicate that the codifications can predict fatigue lives accurately within a factor of 2, when fatigue life is lower than 60,000 cycles. After these cycles, the experimental fatigue lives are much lower than the prediction (up to factor of 20), indicating that both models are not necessarily conservative for this material in the high cycle fatigue region.

It could be possible to increase the accuracy of the F_{en} prediction by using the best-fit lines considering the strain hardening level.

Figure 17 and **Figure 18** compare the experimental F_{en} and the predicted F_{en} with NUREG 6909 and the JSME codification, revealing that both models can predict F_{en} with good accuracy of factor of 2. However, it can be also pointed out that the JSME model tends to give conservative prediction on the cold-worked material, the NUREG model seems less conservative on the as-received material.
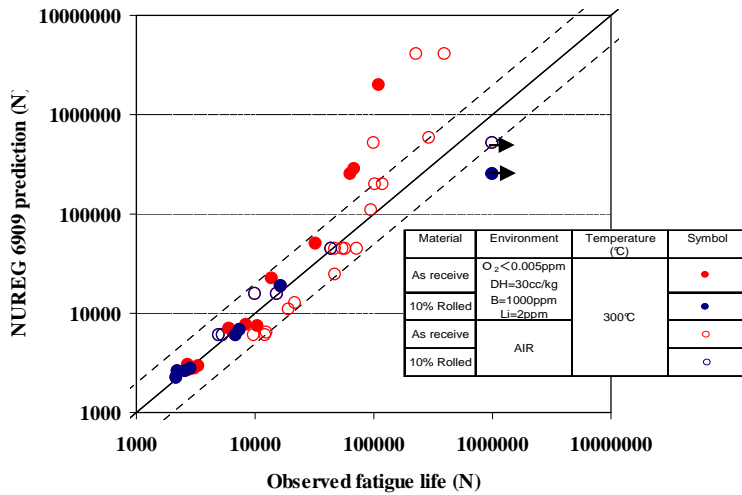
8 Copyright © 2012 by ASME

Figure 15 – Comparison between NUREG 6909 fatigue life prediction and experimental fatigue life.
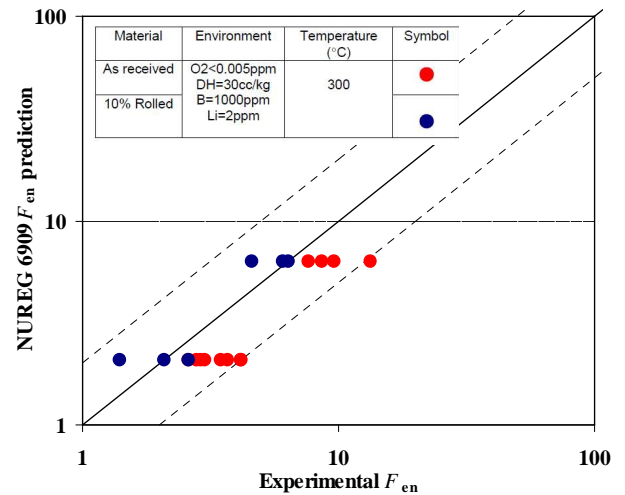

Figure 17 - Comparison between NUREG 6909 F_{en} prediction and experimental F_{en}.
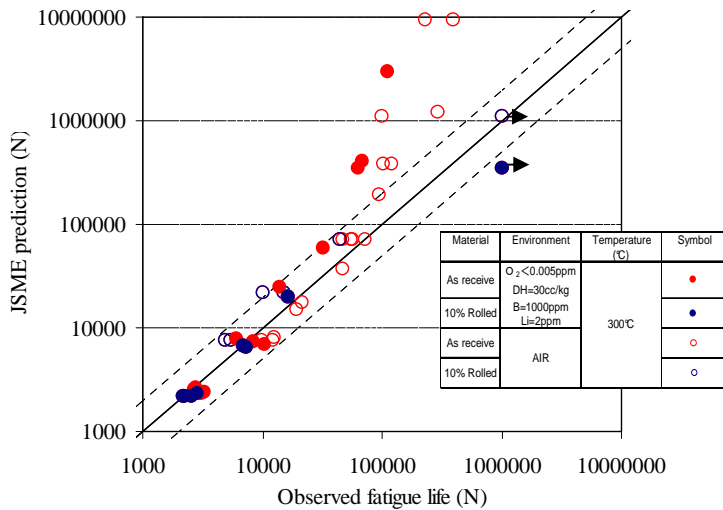

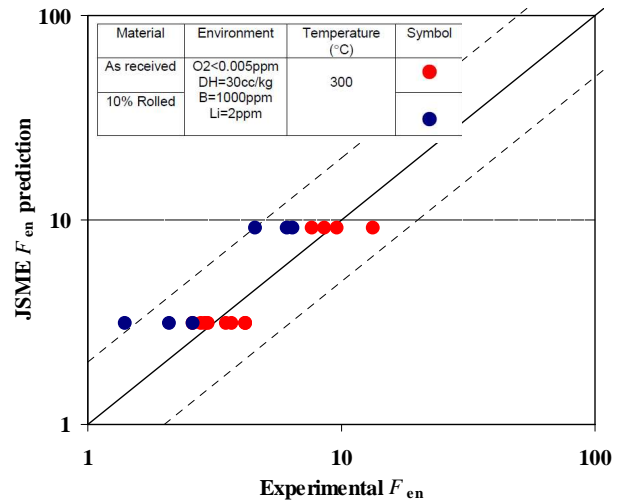**Figure 16 – Comparison between JSME fatigue life prediction and experimental fatigue life.**

Figure 18 – Comparison between JSME F_{en} prediction and experimental F_{en}.

CONCLUSION

The low cycle fatigue tests with the strain hardened material, 304LSS drew the following conclusions.

✓ The 10% strain hardening on the stainless steel 304L leads to reduction of fatigue life in air, but not in PWR primary water irrespective of strain rate. Therefore, it can be said that the prior hardening up to 10% strain does not cause the negative effect on fatigue life.
✓ The fatigue limit defined at 10^6 cycles of the hardened material increased compared to that of the as-received material in air and in primary water. This suggests that the

9   Copyright © 2012 by ASME

environmental effect could become small when strain amplitude is small, so that increasing of the yield stress due to the prior hardening can lead to a slight rise in the fatigue limit.

✓ Fracture surface observations reveal that crack paths were only TG even at the low strain rate on the hardening material.

✓ Effect of the mean stress on the hardened material was highly affected by the temperature during test; it was observed at room temperature, but not clearly at 300 °C.

✓ As for the mechanical behavior of the materials in primary water, the as-received material showed the hardening in the beginning of cycles and then followed by the softening. On the contrary, the prior hardened material only showed the softening. This phenomenon seemed to be affected by strain rate.

ACKNOWLEDGMENTS

REFERENCES

[1] Chopra, O. K. and Shack, W. J., 2007, "Effect of LWR Coolant Environments on the Fatigue Life of Reactor Materials," Final Report, NUREG/CR-6909, ANL-06/08.

[2] Japan Society Mechanical Engineers, 2006, Codes for Nuclear Power Generation Facilities, "Environmental Fatigue Evaluation Method for Nuclear Power Plants," JSME S NF1-2006. (Japanese)

[3] Francois Vaillant, et al., 2009, "Stress Corrosion Cracking Propagation of Cold–worked Austenitic Stainless Steels in PWR Environment," 14th Int. Conf. on Environmental Degradation of Materials in Nuclear Power Systems.

[4] T. Couvant, et al., 2009, "Development of Understanding of the Interaction Between Localized Deformation and SCC of Austenitic Stainless Steels Exposed to Primary PWR Environment," 14th Int. Conf. on Environmental Degradation of Materials in Nuclear Power Systems.

[5] H.D. Solomon, et al., 2005, "Comparison of the fatigue life of type 304L SS as measured in load and strain controlled tests," 12th Int. Conf. on Environmental Degradation of Materials in Nuclear Power Systems.

[6] S. Ganesh Sundara Raman and K.A. Padmanabhan, 1996, "Effect of prior cold work on the room-temperature low-cycle fatigue behavior of AISI 304LN stainless steel", Int. J. Fatigue Vol.18, No.2, pp.71-79.